ACS Macro Letters

Letter

pubs.acs.org/macroletters

Mussel-Glue Derived Peptide–Polymer Conjugates to Realize Enzyme-Activated Antifouling Coatings

Patrick Wilke and Hans G. Börner*

Laboratory for Organic Synthesis of Functional Systems, Department of Chemistry, Humboldt Universität zu Berlin, Brook-Taylor-Str. 2, 12489 Berlin, Germany

Supporting Information

ABSTRACT: Enzyme-activated polymer coatings based on peptide–polymer conjugates are described. Tyrosinase is used to "switch on" adhesive functions of a mussel-glue derived peptide segment, leading to bioconjugates that adhere to steel. The coating resists seawater treatments and modulates surface properties to antifouling surfaces by strongly reducing protein adsorption.

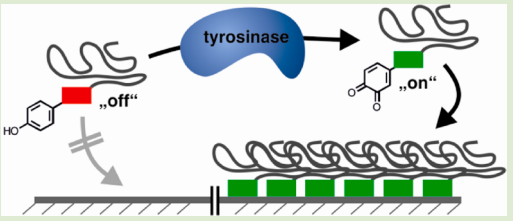

The adhesive system of marine mussels stimulated intensive interdisciplinary research.[1−6] Mussels adhere onto virtually any hard substrate in hostile environments under high salt and strong sheer conditions.[3] The generated mechanical–chemical interfaces are highly purpose adapted and outperform in many aspects properties of technical wet-glues. While the history of studies on related enzymatic processes, for example, the melanin biosynthesis, dates back to the early 1900,[7] in the last decades, Waite et al. revealed the biochemical and biomaterial background of mussel adhesion.[3,8−10] In mussel glues, 3,4-dihydroxy-L-phenylalanin (DOPA) proved to play multiple key roles during adhesion.[11,12] Besides generating the chemical interface to the substrate, the mussel forms DOPA cross-links between mussel foot proteins (mfp), which also strengthen cohesion in the foot plaque.

Yamamoto et al. pioneered in the field of mussel-glue inspired polymers.[13−15] The adhesion of segmented copolymers was studied, which exhibited repeats of sequences containing DOPA/L-lysine (Lys) or octapeptides derived from adhesive proteins. Deming et al. investigated the adhesion of high molecular weight poly(DOPA-*co*-Lys).[16,17] In these studies, cross-linking of the polymers was triggered by chemical or enzymatic oxidation and remarkably increased cohesion. Messersmith et al. exploited highly successful the potential of DOPA for various material science applications.[18−21] Poly(ethylene oxide) was anchored by $(DOPA)_{1-3}$ or DOPA containing peptides to substrates, generating antifouling coatings.[22,23] More recently, effective shielding was achieved by Textor et al., anchoring ethylene-glycol dendrons by $(DOPA)_{1-3}$ to titania.[24]

Obviously, DOPA containing oligo- and polymers proved to offer tremendous opportunities for under-water adhesives.[3,5] However, especially under nonacidic conditions, the catechol DOPA is prone to side reactions[25,26] that might reduce ease of applicability. Mussels detour this difficulty with precursor proteins containing stable tyrosine (Tyr) residues. Specific phenol oxidases, for example, tyrosinases, process these Tyr precursors, leading on demand to peptides with DOPA.[3] While much is known on mfp's derived peptides that can be processed by tyrosinases,[27,28] an enzymatically activated coating has not been described, yet.

Recently, functions of peptide–polymer conjugates were regulated by various means such as pH, Ca^{2+} levels, or enzymes.[29−32] Particularly the latter exhibits high selectivity, making enzymatic processing of peptide segments in bioconjugates valuable tools for specific material science applications.

Here, we present a study on enzymatically activated antifouling coatings to overcome some limitations of DOPA-containing polymers. Poly(ethylene oxide)–peptide conjugates, which exhibit precursor adhesion peptides, show minor adhesive properties to stainless steel. The peptide segment fulfills requirements for tyrosinase substrates and can be enzymatically processed to activate adhesion properties (cf., Figure 1).

The *Mytilus edulis* foot protein mefp-1 is an abundant primer protein, which modulates the adhesion between substrates and the bulk of the mussel food-plaque in the interplay with a set of mefp proteins.[33] Waite et al. isolated and studied the minimal adhesive sequence AKPSYPPTYK (**I**) as an important functional section of mefp-1.[27,34] Although this protein does not directly interact with the surface the mussel adheres too, **I** constitutes a substrate for tyrosinase and proved to participate in multiple tasks in the mussel adhesion process.

To investigate the influence of a conjugated polymer chain on the substrate characteristics, the minimal adhesion sequence **I** and the corresponding AKPSYPPTYK–poly(ethylene oxide) conjugate (**II**) with $M_{n,PEO}$ = 3200 (M_w/M_n = 1.06) were synthesized by solid-phase supported peptide synthesis (SPPS). Both the peptide and the bioconjugate could be isolated in a

Received: May 23, 2012
Accepted: June 18, 2012
Published: June 26, 2012

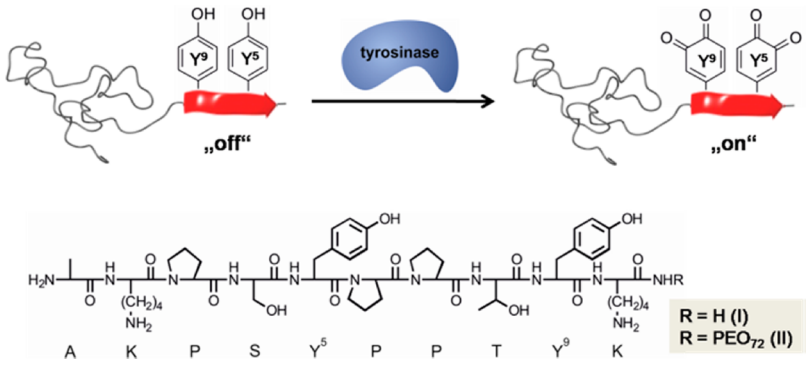

Figure 1. Illustration of the enzymatic activation of a peptide−polymer conjugate, generating DOPA-quinone residues which strongly improve adhesive properties (top) and chemical structure of the mefp-1 derived peptide (**I**) and the corresponding bioconjugate (**II**).

fully deprotected manner and characterization by means of mass spectrometry (ESI-MS, MALDI-TOF-MS) and ^{1}H NMR proved the chemical identities (cf., SI). **I** and **II** were readily soluble in potassium phosphate buffer at pH 6.5 and UV−vis spectroscopy could be used to directly access differences in enzymatic activation kinetics. The generation of DOPA containing species, which exhibited catechol or its derivatives could be followed by reading absorption of the reaction mixtures at 280 nm. Figure 2 suggests for both substrates a

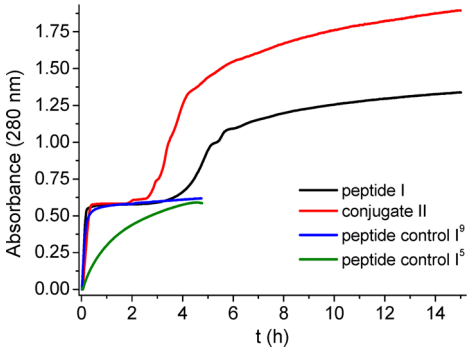

Figure 2. UV-kinetics plot of the tyrosinase-catalyzed oxidation of peptide **I**, bioconjugate **II**, and control peptides I9 and I5 at 280 nm (17 mM buffer, pH 6.5, 100 u tyrosinase and ascorbic acid).

distinct two-step oxidation process. While a first step seems to take place rapidly within ∼20 min, the second step proceeded in 2.5−5 h. Interestingly, the first oxidation step occurs rather independently of the substrate, whereas the second step of **I** was significantly slower compared to that of **II**. To gain insight into this counterintuitive fact, a set of drawn samples along the course of the oxidation processes has been investigated by MALDI-TOF mass spectrometry (cf., SI, Figures S6−9). Apparently, enzymatic oxidation of both **I** and **II** leads rapidly to mono-oxidation products, where one tyrosine residue of the decapeptide was oxidized to DOPA-quinone. Absorption results show only minor changes during the following approximately 2 h, indicating that the resulting species were rather stable upon further enzymatic oxidation. MALDI-TOF-MS measurements at 50 min reaction time indicated the dominant formation of mono-oxidation products for **I** and **II** (cf., SI, Figures S6,7). After ∼2.5 h, UV-absorption rises again, suggesting the oxidation of the second tyrosine. Although reaction rates are different for the activation of **I** and **II**, MALDI-TOF-MS proved a rather effective transformation of the second tyrosine into DOPA-quinone. Under the given conditions the observed oxidation pathway was expected. The resulting species can partially multimerize by forming quinone-amine cross-links as evident also from MS data of **I** and **II** (cf., SI, Figures S7,9).[34]

Considering the specificity of tyrosinase and the different positions of the two tyrosine residues in the peptide segments (Y^5 and Y^9), a two-step oxidation was expected. Earlier studies of enzymatic oxidation of **I** revealed that Y^9 was oxidized approximately 5-times more often than Y^5.[27] To assign the two different products formed in the kinetic study to the distinct tyrosine residues, a serine scan was performed. For that purpose, Tyr residues of the peptide were systematically exchanged by serine (S), which could not participate in the oxidation process. The kinetics of the enzymatic activation of sequence derivatives AKPS**S**PPT$\underline{Y^2}$K (**I**^{9}) and AKPS$\underline{Y^5}$PPT**S**K (**I**^{5}) were investigated by UV−vis spectroscopy (Figure 2). Reaction rates occurred faster for the Tyr^9 bearing peptide compared to that of the Tyr^5 analogue. Consistent with the enzymatic activation of **I**, the absorption at 280 nm during **I**^{9} activation levels off rapidly after ∼30 min at approximately 0.6 au. **I**^{5} activation reached a maximum of ∼0.6 au during ∼4.5 h. Apparently, the oxidation processes of Y^9 and Y^5 were not coupled. However, Y^9 shows much better tyrosinase substrate characteristics. It seems to be likely, that the first oxidation step of **I** and **II** involves a fast enzymatic activation of Y^9 followed by a delayed oxidation of Y^5 in a second, slower step. The visible delay in Y^5 oxidation, which occurred during **I** and **II** activation might be explained by a temporary lag phase. Due to the fact that Y^9 is a better substrate for tyrosinase than Y^5, it is likely that the displacement of the oxidized Y^9 from the catalytic center of the enzyme by the weaker Y^5 substrate might be slow.

Detailed comparison of the oxidation kinetics of **I** and **II** revealed interesting tendencies (cf., Figure 2). The first oxidation step proceeded rather similar with both substrates and both reactions reached UV-absorption values of 0.6 au. Only minor differences were visible as the bioconjugate activation occurred slightly slower compared to that of the nonconjugated peptide. Apparently, the PEO-chain does not interfere dramatically with substrate-enzyme recognition or oxidation of Y^9. Interestingly, conversion of the Y^5 residue proceeded in a different manner. Contrary to the first step, the onset of oxidation appeared earlier and the rate of activation was faster for the bioconjugate oxidation, compared to the nonconjugated peptide. Obviously, PEO conjugation has only an effect on the second oxidation step. This might be rationalized by the fact that PEO could enhance the dissociation of the oxidized Y^9 from the catalytic center of

dx.doi.org/10.1021/mz300258m | *ACS Macro Lett.* 2012, 1, 871−875

tyrosinase, improving displacement of the oxidized Y^9 with the Y^5 substrate and reducing the lag phase for the second oxidation step.

To prove feasibility of an enzyme-activated coating, the adhesion properties of the bioconjugate (**II**) toward stainless steel substrates were investigated before and after enzymatic oxidation. Quartz crystal microbalance (QCM) measurements were carried out with steel-coated probes, studying the deposition and coating stability of **II** and its activated DOPA-quinone dioxidized product ($\mathbf{II}^{2ox}$) from aqueous solutions.

Figure 3 compares the initial adhesion traces of **II** and $\mathbf{II}^{2ox}$ in buffer onto conditioned steel substrates, followed by rinsing the

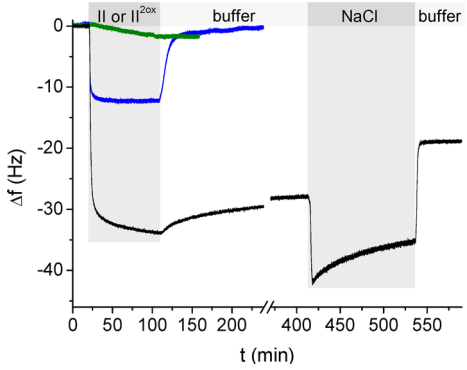

Figure 3. QCM adsorption and desorption kinetics of nonactivated conjugate **II** (blue), the DOPA-quinone activated dioxidized conjugate $\mathbf{II}^{2ox}$ (black) and tyrosinase control (green). Conditions: Buffer equilibrated steel substrates were exposed to conjugate solutions and rinsed with 0.8 mM potassium phosphate buffer. To test stability against seawater, the coating was rinsed with a solution of 599 mM NaCl, followed by buffer, for end-point estimation.

resulting surface coatings with buffer. Clear differences can be observed. Where **II** adhered to steel in a practically fully reversible manner, DOPA-quinone-activated bioconjugate ($\mathbf{II}^{2ox}$) rapidly leads to a stable coating. The amount of adhered compound is in first approximation proportional to the change in frequency of the resonator crystal. Thus, the equilibrium frequency differences of −12 Hz (**II**) and −34 Hz ($\mathbf{II}^{2ox}$) indicated a significantly higher material deposition reached during initial adsorption of the enzyme-activated bioconjugate $\mathbf{II}^{2ox}$ compared to the nonactivated compound. Furthermore, a layer thickness of approximately 6 nm could be calculated for the $\mathbf{II}^{2ox}$ coating, applying the Voigt model.[35] This coat thickness suggests a more mushroom-like conformation, as low chain grafting densities could be expected under the given conditions. As an almost complete removal of the coating of **II** was achieved simply by 30 min of washing the coated metal surface with buffer, the nonactivated bioconjugate represents a very weak, reversible steel binder. The control experiment exposed the sensor to a solution of PEO, enzyme, and ascorbic acid. Figure 3 only shows a minor frequency change of −2 Hz, implying that these components were not significantly contributing to the coating. The remarkable increase in adhesion strength between **II** and $\mathbf{II}^{2ox}$ is noteworthy as this would be expected from the corresponding catechol derivative, but not necessarily from the quinone.[12] To exclude a redox-reaction on the steel surface, which might generate strong binding catechol groups, control experiments on aluminum oxide were performed. Similar results were obtained in these systems, where a redox-reaction is very unlikely to occur (data not shown).

These findings highlight the elegance of a biologically derived coating. The byssal foot proteins, for example, mefp-1, proved to be strong adhesives for all kinds of surfaces.[23,26] However, the respective precursor proteins exhibit a down-regulated function and require activation by specific enzymes. Indeed, some aspects of this complex and highly tailored bioadhesion process could be mimicked by the biologically inspired bioconjugate.

It is noteworthy that mussel adhesion stands harsh conditions of seawater, which is a challenge for many coatings. Ultimate proof for adhesion of an advanced under-water coating is, therefore, the exposure to seawater. For that purpose, a subsequent washing step was carried out with 599 mM NaCl, representing the salt concentration of seawater (cf., Figure 3, 245−370 min).[36] Rinsing the steel substrate coating of $\mathbf{II}^{2ox}$ with a solution of high salt concentration initially leads to a decrease in frequency, which is probably due to salt insertion into the coating. Most importantly, however, is the fact that, after ∼2 h of saltwater rinsing, a subsequent washing step with standard buffer solution reveals a remaining ∼70% of the activated bioconjugate coating. The sensor frequency rises to −19 Hz, suggesting the stability of a significant amount of coating material and highlighting the strong steel binding properties of DOPA-quinone activated peptide−polymer conjugates.

PEO coatings are discussed to exhibit enormous potentials in a broad range of applications from increase of biocompatibility of implants towards reduction of biofouling for hull protection of static vessels.[37] To demonstrate the function of $\mathbf{II}^{2ox}$ as an effective coating for steel, the properties to reduce or even prevent protein adsorption were studied (Figure 4). Besides evaluation of the coating for potential applications, also indirect insight into the surface coverage and the stability of the produced coating were obtained. Coated and noncoated steel surfaces were exposed to solutions of 10 mg/mL bovine serum albumin (BSA), and QCM measurements enabled to follow the protein adsorption process. Figure 4A shows a clear effect of the coating in reducing BSA adsorption on steel substrates and rendering protein adhesion reversible. Where initial protein adsorption leads to a frequency reduction of −32 Hz within an hour on noncoated steel substrates, a change of only −8 Hz was evident during the same time period if BSA solutions are exposed to coated surfaces. Even more important, the coated surface returned almost to the frequency of the initial coating after rinsing both surfaces with buffer, suggesting practically fully reversible interactions of BSA with coated steel. Instead, the control experiment leads to a frequency of −22 Hz, indicating a significant amount of adhered BSA.

While BSA represents a defined model system, exposing coated and noncoated steel surfaces to human full blood serum allows for studying a complex protein mixture, which is closer to applications. Figure 4B confirms also in this case a clear reduction of serum adsorption on coated steel surfaces. Whereas the exposure on bare steel substrates leads to frequency changes of −64 Hz within 1 h, only a −10 Hz shift was observed for the coated surface. Furthermore, the frequency for the coated steel surface returned to −6 Hz upon rinsing with water, while the reference experiment showed a rather stable protein layer with −45 Hz. Certainly, some room for optimization is still given. However, the enzyme-activated

dx.doi.org/10.1021/mz300258m | ACS Macro Lett. 2012, 1, 871−875

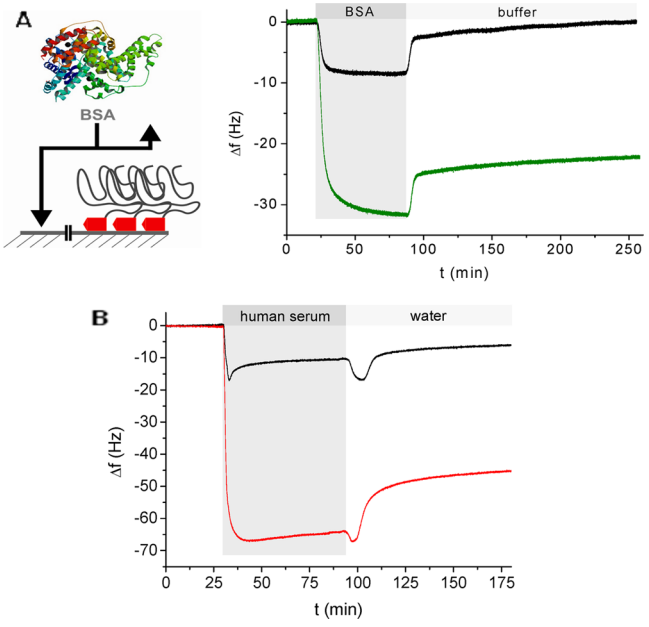

Figure 4. (A) Illustration of the BSA adsorption onto coated and noncoated substrates (left) and QCM adsorption kinetics of an antifouling experiment (right) showing BSA adsorption onto $\mathbf{II}^{2ox}$ coatings (black) and noncoated steel (green). (B) Antifouling experiment with human full blood serum adsorption onto $\mathbf{II}^{2ox}$ coatings (black) and noncoated steel (red). Conditions: Equilibrated $\mathbf{II}^{2ox}$ coatings and steel substrates were exposed to BSA or blood serum solutions, followed by rinsing for end point estimation; BSA structure: PDB 3V03.

quinone coating effectively reduced the adhesion of proteins by peptide-mediated attachment of PEO.

In summary, the conjugation of poly(ethylene oxide) (PEO) to a decapeptide that has been derived from a native mussel coat protein resulted in a functional bioconjugate, which could be enzymatically activated by tyrosinase. A distinct two-step oxidation reaction activates the peptide sequence by transforming two Tyr residues into 3,4-dihydroxy-L-phenylalanine derivatives (DOPA-quinone). This up-regulates the adhesive properties of the bioconjugate from reversible weak steel binder to a strong, adhesive to steel substrates, as shown by quartz crystal microbalance measurements (QCM). The coating is robust to dilution and even defeats rather well rinsing with seawater model solutions of c[NaCl] ~ 0.6 mol. The coating exhibits PEO, which is attached via peptide-mediated noncovalent substrate binding. A significant reduction of protein adsorption (human full blood serum and bovine serum albumin) on the coated substrates revealed potential antifouling properties. The biomimetic system realized an enzymatically triggered coating. The stable precursor bioconjugate was not suffering from a lack of stability as the sensitive DOPA residues were produced in situ, prior to the coating, which paves the way for developments of practical enzyme-activated DOPA-quinone glues or coatings.

■ ASSOCIATED CONTENT

Supporting Information

Experimental procedures as well as analytical data for all compounds and detailed QCM data. This material is available free of charge via the Internet at http://pubs.acs.org.

■ AUTHOR INFORMATION

Corresponding Author

*E-mail: h.boerner@hu-berlin.de. Phone: (+49) 30-2093-7348. Fax: (+49) 30-2093-7500.

Notes

The authors declare no competing financial interest.

■ ACKNOWLEDGMENTS

The authors acknowledge Dr. Steffen Weidner (BAM-Berlin) for MALDI-TOF-MS measurements and Katharina Linkert (HU Berlin) for peptide and conjugate synthesis. Financial support was granted by the German Research Council DFG (BEKs BO1762/5-1).

■ REFERENCES

(1) Waite, J. H.; Tanzer, M. L. *Science* **1981**, *212*, 1038.
(2) Waite, J. H. *Int. J. Adhes. Adhes.* **1987**, *7*, 9.
(3) Lee, B. P.; Messersmith, P. B.; Israelachvili, J. N.; Waite, J. H. *Annu. Rev. Mater. Res.* **2011**, *41*, 99.
(4) Lee, H.; Dellatore, S. M.; Miller, W. M.; Messersmith, P. B. *Science* **2007**, *318*, 426.
(5) Brubaker, C. E.; Messersmith, P. B. *Langmuir* **2012**, *28*, 2200.
(6) Metzke, M.; Bai, J. Z.; Guan, Z. B. *J. Am. Chem. Soc.* **2003**, *125*, 7760.
(7) Raper, H. S.; Wormall, A. *Biochem. J.* **1923**, *17*, 454.
(8) Waite, J. H.; Housley, T. J.; Tanzer, M. L. *Biochemistry* **1985**, *24*, 5010.
(9) Coyne, K. J.; Qin, X. X.; Waite, J. H. *Science* **1997**, *277*, 1830.
(10) Harrington, M. J.; Masic, A.; Holten-Andersen, N.; Waite, J. H.; Fratzl, P. *Science* **2011**, *328*, 216.
(11) Anderson, T. H.; Yu, J.; Estrada, A.; Hammer, M. U.; Waite, J. H.; Israelachvili, J. N. *Adv. Funct. Mater.* **2011**, *20*, 4196.
(12) Lee, H.; Scherer, N. F.; Messersmith, P. B. *Proc. Natl. Acad. Sci. U.S.A.* **2006**, *103*, 12999.
(13) Yamamoto, H.; Hayakawa, T. *Polymer* **1978**, *19*, 1115.
(14) Yamamoto, H.; Hayakawa, T. *Macromolecules* **1983**, *16*, 1058.
(15) Yamamoto, H. *J. Chem. Soc., Perkin Trans. 1* **1987**, 613.
(16) Yu, M. E.; Deming, T. J. *Macromolecules* **1998**, *31*, 4739.
(17) Yu, M. E.; Hwang, J. Y.; Deming, T. J. *J. Am. Chem. Soc.* **1999**, *121*, 5825.
(18) Su, J.; Chen, F.; Cryns, V. L.; Messersmith, P. B. *J. Am. Chem. Soc.* **2011**, *133*, 11850.
(19) Lee, H.; Lee, B. P.; Messersmith, P. B. *Nature* **2007**, *448*, 338.
(20) Lee, B. P.; Dalsin, J. L.; Messersmith, P. B. *Biomacromolecules* **2002**, *3*, 1038.
(21) Huang, K.; Lee, B. P.; Ingram, D. R.; Messersmith, P. B. *Biomacromolecules* **2002**, *3*, 397.
(22) Dalsin, J. L.; Lin, L. J.; Tosatti, S.; Voros, J.; Textor, M.; Messersmith, P. B. *Langmuir* **2005**, *21*, 640.
(23) Dalsin, J. L.; Hu, B. H.; Lee, B. P.; Messersmith, P. B. *J. Am. Chem. Soc.* **2003**, *125*, 4253.
(24) Gillich, T.; Benetti, E. M.; Rakhmatullina, E.; Konradi, R.; Li, W.; Zhang, A.; Schluter, A. D.; Textor, M. *J. Am. Chem. Soc.* **2011**, *133*, 10940.
(25) Brunmark, A.; Cadenas, E. *Free Radical Biol. Med.* **1989**, *7*, 435.
(26) Lin, Q.; Gourdon, D.; Sun, C.; Holten-Andersen, N.; Anderson, T. H.; Waite, J. H.; Israelachvili, J. N. *Proc. Natl. Acad. Sci. U.S.A.* **2007**, *104*, 3782.
(27) Marumo, K.; Waite, J. H. *Biochim. Biophys. Acta* **1986**, *872*, 98.
(28) Suci, P. A.; Geesey, G. G. *J. Colloid Interface Sci.* **2000**, *230*, 340.
(29) Hentschel, J.; Krause, E.; Börner, H. G. *J. Am. Chem. Soc.* **2006**, *128*, 7722.
(30) Hentschel, J.; Bleek, K.; Ernst, O.; Lutz, J.-F.; Börner, H. G. *Macromolecules* **2008**, *41*, 1073.
(31) Kühnle, R. I.; Börner, H. G. *Angew. Chem., Int. Ed.* **2011**, *50*, 4499.
(32) Kühnle, H.; Börner, H. G. *Angew. Chem., Int. Ed.* **2009**, *48*, 6431.

(33) Holten-Andersen, N.; Waite, J. H. *J. Dent. Res.* **2008**, *87*, 701.
(34) Burzio, L. A.; Waite, J. H. *Biochemistry* **2000**, *39*, 11147.
(35) Weber, N.; Wendel, H. P.; Kohn, J. *J. Biomed. Mater. Res., Part A* **2005**, *72A*, 420.
(36) Sharqawy, M. H.; Lienhard, J. H.; Zubair, S. M. *Desalin. Water Treat.* **2010**, *29*, 355.
(37) Banerjee, I.; Pangule, R. C.; KaneIndrani, R. S. *Adv. Mater.* **2011**, *23*, 690.